JACS
JOURNAL OF THE AMERICAN CHEMICAL SOCIETY
Communication
pubs.acs.org/JACS

"Smart" Ag Nanostructures for Plasmon-Enhanced Spectroscopies

Chao-Yu Li,[†] Meng Meng,[†] Sheng-Chao Huang,[†] Lei Li,[§] Shao-Rong Huang,[†] Shu Chen,[‡] Ling-Yan Meng,[‡] Rajapandiyan Panneerselvam,[†] San-Jun Zhang,[§] Bin Ren,[†] Zhi-Lin Yang,[‡] Jian-Feng Li,*[,†] and Zhong-Qun Tian[†]

[†]MOE Key Laboratory of Spectrochemical Analysis and Instrumentation, State Key Laboratory of Physical Chemistry of Solid Surfaces, College of Chemistry and Chemical Engineering, and [‡]Department of Physics, Xiamen University, Xiamen 361005, China
[§]State Key Laboratory of Precision Spectroscopy, East China Normal University, Shanghai 200062, China

Supporting Information

ABSTRACT: Silver is an ideal candidate for surface plasmon resonance (SPR)-based applications because of its great optical cross-section in the visible region. However, the uses of Ag in plasmon-enhanced spectroscopies have been limited due to their interference via direct contact with analytes, the poor chemical stability, and the Ag^+ release phenomenon. Herein, we report a facile chemical method to prepare shell-isolated Ag nanoparticle/tip. The as-prepared nanostructures exhibit an excellent chemical stability and plasmonic property in plasmon-enhanced spectroscopies for more than one year. It also features an alternative plasmon-mediated photocatalysis pathway by smartly blocking "hot" electrons. Astonishingly, the shell-isolated Ag nanoparticles (Ag SHINs), as "smart plasmonic dusts", reveal a ~1000-fold ensemble enhancement of rhodamine isothiocyanate (RITC) on a quartz substrate in surface-enhanced fluorescence. The presented "smart" Ag nanostructures offer a unique way for the promotion of ultrahigh sensitivity and reliability in plasmon-enhanced spectroscopies.

Ag nanostructures, with the excellent SPR properties, are considered to be a fascinating substrate for ultrasensitive analyses down to the single-molecule level in surface-enhanced Raman scattering (SERS),[1] and also commonly used as the scanning probe microscopy (SPM) tip for the chemical imaging with a nanoscale spatial resolution in tip-enhanced Raman scattering (TERS).[2] It is also attractive for plasmon-enhanced fluorescence. However, there are several factors that should be taken into consideration when the bare Ag nanostructures are used: (i) the probes/analytes are in direct contact with the silver surface and can cause an interference in the spectroscopic analysis; (ii) in SPR-mediated chemical reactions, the mechanisms are complex due to the dual functions of Ag nanostructures as local electric field amplifiers and as "hot carrier" donors;[2b,3] and (iii) Ag can be easily oxidized under ambient conditions, which is a bottleneck for its applications and leads to a significant decrease in the plasmonic enhancement.[3c,4] Importantly, Ag^+ ions that are released from silver NPs occur even in a hypoxic condition, and adsorbed Ag^+ will transform to oxides in an alkaline environment or may interact with the atmospheric sulfur-containing compounds to form sulfides.[5]

To improve the plasmonic performance of silver nanostructures, extensive efforts have been devoted to synthetic methodologies,[6] such as covering silver nanoparticle (NP) with graphene[6b,c] and introducing Au to prepare bimetallic NPs.[6a,d] However, the substrate generality issue is not solved because of the immobile property of the plasmonic substrate,[6c] the interference from the background signals of the graphitic shell,[6b,c] and the poor plasmonic performance below ~530 nm due to the interband transition of Au.[6a,d] Therefore, it is necessary to utilize a chemically inert and optically transparent material as a coating shell, such as silica, to fulfill the above-mentioned requirements.[7] To obtain accurate information during spectroscopic analysis, the silica shell should be free of pinholes; otherwise, the target analytes or contaminants can directly interact with the Ag core and generate strong interferential or misleading SERS signals. However, the silica shell prepared via the traditional Stöber method is porous and cannot protect the Ag surface from corrosion and the direct contact with probes/analytes.[7a]

In 2010, our group invented a novel technique, called "shell-isolated nanoparticle-enhanced Raman spectroscopy" (SHINERS) in which the shell-isolated nanoparticle (SHIN) consists of a gold core and an ultrathin SiO_2 shell.[8] The compact and ultrathin silica shell efficiently transmits the strong electromagnetic enhancement from the gold core and protects the core from the analyte/probed molecules.[9] However, in contrast to Au, it is extremely difficult to avoid the formation of Ag_2O or Ag_2S during the chemical synthesis of $Ag@SiO_2$. The released Ag^+ will retard the coating due to the further formation of sulfides/oxides on the Ag NP surface.[5] Thus, it is still highly desirable to develop a method to prepare pinhole-free shell-isolated Ag nanostructures for plasmon-enhanced spectroscopies.

Herein, we introduce a facile chemical method to prepare shell-isolated Ag nanostructures by a simple treatment with $NaBH_4$ under ambient conditions, which requires neither deoxygenation systems nor expensive instruments. The as-prepared Ag SHINs exhibit remarkable plasmon-enhancing capabilities with high stability even after 16 months of storage. This method also works for shell-isolated tip-enhanced Raman spectroscopy (SITERS), showing the capability of smartly blocking "hot" electrons in plasmon-mediated reactions. Finally,

Received: September 15, 2015
Published: October 20, 2015

DOI: 10.1021/jacs.5b09682
J. Am. Chem. Soc. 2015, 137, 13784−13787

by simply spreading the "smart plasmonic dusts" on a RITC-functionalized quartz substrate, a strong ensemble enhancement (~1000-fold) can be obtained.

Ag nanospheres with a diameter of 96 nm were synthesized using a seed growth method. The concentration of the released Ag^+ from the Ag NPs in the as-prepared sol was measured with an ion selective electrode to be 1.09 μg/mL (0.8 wt %). Based on the thermodynamic analysis, Ag^0 will not be persistent in realistic conditions that contain trace amounts of dissolved oxygen, and then Ag^+ release occurs.[5a] Thus, $NaBH_4$ treatment was introduced in our preparation to reduce the surface-adsorbed Ag^+ species. The extinction spectra in Supporting Information Figure S1 depict the role of $NaBH_4$ in retaining the activity of the Ag NPs. The interaction between the fresh silver surface and the silane coupling agent, (3-aminopropyl)trimethoxysilane (ATPMS), was facilitated by the $NaBH_4$ treatment. Thus, a compact and ultrathin silica shell was uniformly coated on silver. As shown in Figures 1B and S2, Ag SHINs with a silica shell

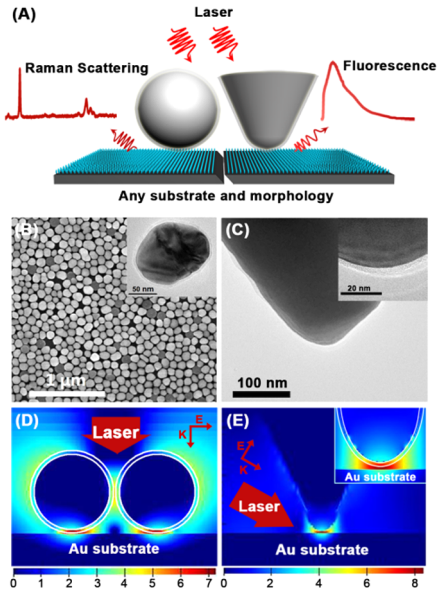

Figure 1. (A) Schematic diagram of "smart" Ag nanostructure-enhanced spectroscopies. (B) SEM image of Ag SHINs with a 4 nm shell. Inset: HR-TEM image of a single Ag SHINs. (C) TEM image of a Ag tip coated with 1–2 nm of SiO_2. Inset: HR-TEM image of sharp tip end. (D) Three-dimensional FDTD simulation of four Ag SHINs (2 × 2 array) on a gold substrate (side-view) excited at 638 nm. (E) Three-dimensional FDTD simulation of a nanocavity formed by a silica-coated Ag tip and a Au substrate that is illuminated from the side at an angle of 60° (633 nm). The shell thickness, tip–substrate distance, tip radius, and cone angle were set to 2, 1, and 30 nm, and 30°, respectively.

thickness that varied from 2 to 20 nm were obtained using our method. Additionally, Figure S3 clearly shows that the $NaBH_4$ treatment ensures the formation of pinhole-free Ag SHINs even with a smaller Ag core (52 nm diameter, released Ag^+ increased to 3.64 wt % due to higher surface energy). To determine the role of $NaBH_4$, Ag SHINs were prepared under the same conditions without $NaBH_4$, as shown in Figures S3C,D and S4, and the prepared Ag NPs contained many pinholes. When the $NaBH_4$ treatment was absent, the surface oxidation impedes the interaction between the Ag surface and the silane molecules, which results in an uneven silica coating.

To determine the versatility of our method, a shell-isolated TERS tip was also prepared with the $NaBH_4$ treatment. TERS is a powerful surface technique that can provide strong Raman vibrational information with high spatial resolution.[2a−c] However, the formation of Ag_2O/Ag_2S is difficult to avoid when a bare Ag tip is exposed to the atmospheric environment, which induces the loss of TERS activity.[10] Therefore, shell-isolated tip coating method could improve the stability and sensitivity of the TERS under the ambient conditions and protect the tip from the interferences of electrolytes, other species in solution, or even probes at electrochemical interface. Using $NaBH_4$, we successfully prepared a shell-isolated silver tip with a ~2 nm silica shell for the TERS measurements (Figure 1C).

Figure 2a shows the remarkable stability of the shell-isolated Ag NPs in the corrosive environment (6 wt % H_2O_2). The SPR

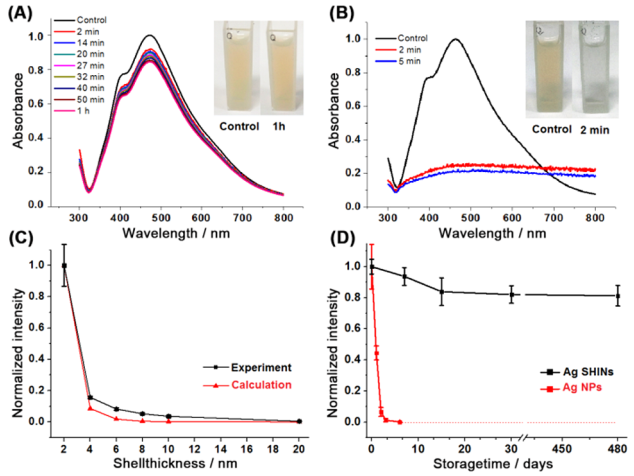

Figure 2. Ultrahigh stability of "smart" Ag SHINs. Time-dependent extinction spectra of (A) Ag SHINs with a 4 nm shell thickness and (B) bare Ag NPs in a 6 wt % H_2O_2 solution. All of the spectral intensities are normalized to the original intensity before H_2O_2 was added (control sample). The insets show the corresponding photographs at different times. (C) The shell thickness dependence on the integrated SHINERS intensity of 10 mM Py (black square) and the corresponding 3D-FDTD calculation result (red triangle). (D) Comparison of the SHINERS intensity of Py on a Ag SHINs coated smooth Ag substrate and on bare Ag NPs after different storage times.

intensity decreased slightly after H_2O_2 injection, while the bare Ag NPs were almost etched within 2 min (Figure 2B). Concurrently, the pinhole-free character of the silica shell is examined with a SERS measurement, and the shell is proven effective for protecting the core from the analytes (see section S2 in SI). Furthermore, the results obtained with the shell-isolated chemical method were compared with the traditional Stöber method. Although the 5 nm silica shell was coated via the hydrolysis of tetraethoxysilane (TEOS), the strong Raman signal of Py was observed in the pinhole test, and the NPs were evidently etched in the H_2O_2 solution (Figure S6). Figure 2c shows the SHINERS intensities of the ν_1 mode (at 1008 cm^{-1}) of pyridine (Py) adsorbed on the smooth Ag substrates modified with Ag SHINs with different silica shell thickness (the corresponding spectra are shown in Figure S7A). As expected, the SHINERS intensity of Py decreases significantly with an increase in the shell thickness.

To investigate the long-term stability of SHINs, Ag NPs and Ag SHINs were stored under ambient conditions for a long period of time. The SERS/SHINERS intensities of the ν_1 mode of Py (10 mM) versus the storage time are plotted in Figure 2D. The decrease in the SERS intensity of the bare Ag NPs is

DOI: 10.1021/jacs.5b09682
J. Am. Chem. Soc. 2015, 137, 13784−13787

significant, and the signal was no longer visible after 5 days of storage. Due to the formation of an oxide/sulfide layer on the Ag NP surface, the losses in the electromagnetic and chemical enhancements are significant.[4] However, with the protection of the ultrathin silica shell, the Ag SHINs exhibits remarkable long-term plasmonic properties (in Figure S7B). Compared with a freshly prepared sample, the decay in the Raman intensity is less than 20% even after 16 months of storage. Because of the outstanding chemical stability and long-term plasmonic property, Ag SHINs are extraordinarily suitable for commercialization and practical applications.

Although Ag is commonly preferred in plasmon-mediated chemical reactions, it is difficult to obtain an exact mechanism due to the multifaceted process.[2b,3a,b,e−g] To elucidate plasmon-mediated reactions, it is necessary to monitor and control the reaction pathways. 4-Aminothiophenol (PATP) is a common probed molecule with a unique SERS signal; however, it is easily oxidized to 4,4′-dimercaptoazobenzene (DMAB) on silver surface under laser illumination.[3c] In conventional Raman measurements, "hot" electrons are excited in Ag NPs and then transferred into the antibonding O−O $2\pi^*$-state of surface-adsorbed O_2 to yield O_2^- anions.[3c,f] The presence of O_2^- anion promotes the formation of metal oxides on the NP surface, which will further oxidize PATP to DMAB.[3c] To achieve controllable chemical transformation of PATP to DMAB, a gap-mode configuration was employed, which consists of an atomically flat Au(111) surface/PATP self-assembled monolayer/nanoparticles. As shown in Figure 3, when bare Ag NPs were cast,

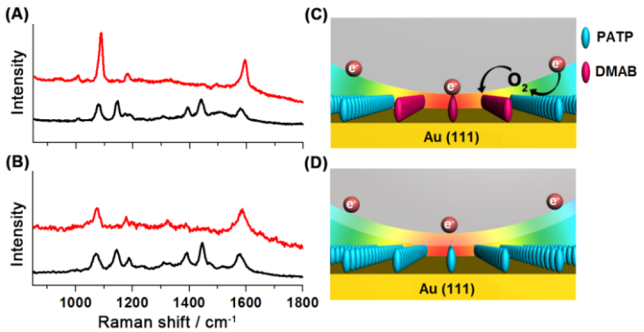

Figure 3. Probing plasmon-mediated chemical reactions by "smart" Ag nanostrustures. (A) SERS spectra of Au(111)/PATP/Ag SHINs (red line) and Au(111)/PATP/Ag NP junctions (black line). (B) TERS spectra of the Au(111)/PATP/silica-coated Ag tip (red line) and the Au(111)/PATP/Ag tip (black line) nanocavities. (C,D) Schematic diagrams of the chemical reaction of PATP to DMAB with the assistance of "hot" electrons in the bare and shell-isolated nanogaps.

PATP transformed to DMAB under 638 nm illumination with the appearance of "b_2 modes" at 1145, 1393, and 1438 cm^{-1}. When Ag NPs were replaced by Ag SHINs (4 nm shell), the chemical transformation of PATP was prevented by the silica shell with the absence of the "b_2 modes", although the illumination power was intensified by 10 times. The same results were obtained when using a 532 nm excitation (Figure S8B).

Furthermore, TERS is also an impressive tool to distinguish the reaction pathways. The photoinduced oxidation of PATP at 633 nm excitation was observed with a Ag tip (Figure 3B),[3d] while the "smart" shell-isolated Ag tip prevented the photocatalytic reaction even though the laser power was intensified by 3 times. The "far field" spectrum when tip was retracted from the surface is shown in Figure S9.

Ag nanostructures play a pivotal role in light harvesting processes by generating "hot" electron−hole pairs, enhancing the local electric field and other mechanisms.[3e,g] This chemical transformation of PATP to DMAB is attributed to the SPR-induced charge transfer mechanism, which is supported by the SHINERS/SITERS results. During our measurements, the SPR-induced charge transfer from Ag NPs to O_2 was uniquely isolated by the ultrathin pinhole-free shell, and the chemical transformation was inhibited. Especially, SITERS is expected to help with further understanding of the influence of tunneling electrons in SPR-mediated reactions.

Shell-isolated Ag nanoparticles inherit the advantage of acquiring a high-quality Raman signal, and they can be further expanded to surface-enhanced fluorescence, which is widely used for biological imaging and sensing.[11] Although silica-coated metal NPs are favorable in plasmon-enhanced fluorescence due to the controllability of the shell thickness for minimizing the nonradiative energy transfer to the metal, it is necessary to improve the average fluorescence enhancement, which is reported typically by 10−20-fold.[9a,11a,12] In this work, RITC molecules were functionalized on a quartz surface via covalent bonding, and SHINs were spread over the RITC film as "smart plasmonic dusts". Figure 4a shows the plasmon-enhanced

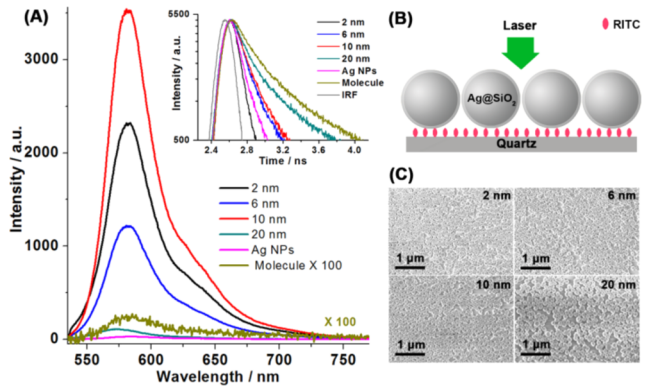

Figure 4. Ultrasensitive surface-enhanced fluorescence using "smart" Ag SHINs. (A) Reference and plasmon-enhanced fluorescence spectra of the RITC film modified by Ag SHINs with different shell thicknesses of 2, 6, 10, and 20 nm, respectively. The inset shows the lifetime measurements. (B) Cartoon diagram of the plasmon-enhanced fluorescence measurement. (C) Corresponding SEM images of the SHINs-RITC film-quartz substrate.

fluorescence spectra with the Ag SHINs and the Ag NPs at an excitation of 532 nm. The background signals from the NPs were corrected in all of the fluorescence spectra, and the NPs-RITC film-quartz substrate configurations were also characterized using SEM (Figure 4C). The fluorescence signal was strongly quenched due to the direct contact with the Ag NPs. However, SHINs exhibited an ensemble enhancement up to about 700-, 370-, 1000-, and 30-fold for the 2, 6, 10, and 20 nm silica shells, respectively. The emission intensity enhancement is simultaneously affected by both the excitation efficiency and quantum yield modification.[11c,e] With the strong confinement of incident light, the excitation efficiency of molecule nearby is prominently improved. Meanwhile, the increased local density of states provides an extra rapid decay channel for emitter, which leads to the modifications of the radiative/nonradiative decay rates and the enhancement of final quantum yield,[11d,f] which is indicated by the increased decay of lifetime as shown in the inset of Figure 4A and section S4. When the shell thickness is 10 nm, the decay

DOI: 10.1021/jacs.5b09682
J. Am. Chem. Soc. 2015, 137, 13784−13787

of lifetime is enhanced by ~25-fold, which means the same enhancement in the emission cyclic rate.[12] Particularly, when the silica shell thickness is optimum (10 nm), the energy dissipation to metal could be minimized and then the huge fluorescence enhancement is obtained.[9a,11a,b] "Smart" Ag SHINs reveal excellent adaptability on diverse substrates for plasmon-enhanced spectroscopies and ultrahigh sensitivity in the spectroscopic analysis. In the near future, SITERS may enhance and control the emission of molecules on a nanometer spatial resolution.

We demonstrated several applications of shell-isolated Ag nanostructures in plasmon-enhanced spectroscopies, which exhibited the ultrahigh stability and the excellent long-term plasmonic performance even after 16 months of storage. SHINERS and SITERS can also be employed to control the photocatalytic reaction pathway of PATP to DMAB. Remarkably, a ~1000-fold enhancement in fluorescence intensity is obtained by simply casting Ag SHINs onto a RITC molecule film. We are optimistic that shell-isolated Ag nanostructures will open up a new avenue in fundamental research and practical applications with great potentials.

■ ASSOCIATED CONTENT

Supporting Information

The Supporting Information is available free of charge on the ACS Publications website at DOI: 10.1021/jacs.5b09682.

Experimental section, TEM/SEM images of SHINs, pinhole and lifetime tests of Ag SHINs, and the time-resolved fluorescence measurements (PDF)

■ AUTHOR INFORMATION

Corresponding Author

*li@xmu.edu.cn

Notes

The authors declare no competing financial interest.

■ ACKNOWLEDGMENTS

We thank Y. L. Zheng, S. Y. Chen, J. H. Gao, C. L. Wu, and J. H. Xu for helpful discussions. This work was supported by Thousand Youth Talents Plan of China, the MOST of China (2011YQ030124), NSFC (21427813), and NFFTBS (No. J1310024).

■ REFERENCES

(1) (a) Nie, S.; Emory, S. R. *Science* **1997**, *275*, 1102. (b) Nie, S.; Zare, R. N. *Annu. Rev. Biophys. Biomol. Struct.* **1997**, *26*, 567. (c) Kneipp, K.; Wang, Y.; Kneipp, H.; Perelman, L. T.; Itzkan, I.; Dasari, R. R.; Feld, M. S. *Phys. Rev. Lett.* **1997**, *78*, 1667. (d) Li, Y.; Jing, C.; Zhang, L.; Long, Y. T. *Chem. Soc. Rev.* **2012**, *41*, 632. (e) Le Ru, E. C.; Etchegoin, P. G. *Annu. Rev. Phys. Chem.* **2012**, *63*, 65.

(2) (a) Pettinger, B.; Picardi, G.; Schuster, R.; Ertl, G. *Electrochemistry* **2000**, *68*, 942. (b) van Schrojenstein Lantman, E. M.; Deckert-Gaudig, T.; Mank, A. J. G.; Deckert, V.; Weckhuysen, B. M. *Nat. Nanotechnol.* **2012**, *7*, 583. (c) Schmid, T.; Opilik, L.; Blum, C.; Zenobi, R. *Angew. Chem., Int. Ed.* **2013**, *52*, 5940. (d) Zhang, R.; Zhang, Y.; Dong, Z. C.; Jiang, S.; Zhang, C.; Chen, L.; Zhang, L.; Liao, Y.; Aizpurua, J.; Luo, Y.; Yang, J. L.; Hou, J. G. *Nature* **2013**, *498*, 82. (e) Sonntag, M. D.; Klingsporn, J. M.; Sharma, B.; Ruvuna, L. K.; Van Duyne, R. P. *Chem. Soc. Rev.* **2014**, *43*, 1230. (f) Domke, K. F.; Zhang, D.; Pettinger, B. *J. Am. Chem. Soc.* **2006**, *128*, 14721. (g) Kawata, S.; Inouye, Y.; Verma, P. *Nat. Photonics* **2009**, *3*, 388. (h) Neacsu, C. C.; Dreyer, J.; Behr, N.; Raschke, M. B. *Phys. Rev. B: Condens. Matter Mater. Phys.* **2006**, *73*, 193406.

(3) (a) Jin, R.; Cao, Y.; Mirkin, C. A.; Kelly, K. L.; Schatz, G. C.; Zheng, J. G. *Science* **2001**, *294*, 1901. (b) Jin, R.; Charles Cao, Y.; Hao, E.; Metraux, G. S.; Schatz, G. C.; Mirkin, C. A. *Nature* **2003**, *425*, 487. (c) Huang, Y. F.; Zhang, M.; Zhao, L. B.; Feng, J. M.; Wu, D. Y.; Ren, B.; Tian, Z. Q. *Angew. Chem., Int. Ed.* **2014**, *53*, 2353. (d) Kumar, N.; Stephanidis, B.; Zenobi, R.; Wain, A. J.; Roy, D. *Nanoscale* **2015**, *7*, 7133. (e) Linic, S.; Christopher, P.; Ingram, D. B. *Nat. Mater.* **2011**, *10*, 911. (f) Christopher, P.; Xin, H.; Linic, S. *Nat. Chem.* **2011**, *3*, 467. (g) Brongersma, M. L.; Halas, N. J.; Nordlander, P. *Nat. Nanotechnol.* **2015**, *10*, 25.

(4) Erol, M.; Han, Y.; Stanley, S. K.; Stafford, C. M.; Du, H.; Sukhishvili, S. *J. Am. Chem. Soc.* **2009**, *131*, 7480.

(5) (a) Liu, J.; Hurt, R. H. *Environ. Sci. Technol.* **2010**, *44*, 2169. (b) Singh, P.; Parent, K. L.; Buttry, D. A. *J. Am. Chem. Soc.* **2012**, *134*, 5610.

(6) (a) Gao, C. B.; Hu, Y. X.; Wang, M. S.; Chi, M. F.; Yin, Y. D. *J. Am. Chem. Soc.* **2014**, *136*, 7474. (b) Song, Z. L.; Chen, Z.; Bian, X.; Zhou, L. Y.; Ding, D.; Liang, H.; Zou, Y. X.; Wang, S. S.; Chen, L.; Yang, C.; Zhang, X. B.; Tan, W. h. *J. Am. Chem. Soc.* **2014**, *136*, 13558. (c) Xu, W.; Ling, X.; Xiao, J.; Dresselhaus, M. S.; Kong, J.; Xu, H.; Liu, Z.; Zhang, J. *Proc. Natl. Acad. Sci. U. S. A.* **2012**, *109*, 9281. (d) Yang, Y.; Liu, J. Y.; Fu, Z. W.; Qin, D. *J. Am. Chem. Soc.* **2014**, *136*, 8153.

(7) (a) Stöber, W.; Fink, A.; Bohn, E. *J. Colloid Interface Sci.* **1968**, *26*, 62. (b) Ung, T.; Liz-Marzán, L. M.; Mulvaney, P. *Langmuir* **1998**, *14*, 3740. (c) Liz-Marzán, L. M.; Mulvaney, P. *J. Phys. Chem. B* **2003**, *107*, 7312. (d) Yin, Y. D.; Lu, Y.; Sun, Y.; Xia, Y. *Nano Lett.* **2002**, *2*, 427. (e) Ge, J.; Zhang, Q.; Yin, Y. *Angew. Chem., Int. Ed.* **2008**, *47*, 8924. (f) Roca, M.; Haes, A. J. *J. Am. Chem. Soc.* **2008**, *130*, 14273.

(8) Li, J. F.; Huang, Y. F.; Ding, Y.; Yang, Z. L.; Li, S. B.; Zhou, X. S.; Fan, F. R.; Zhang, W.; Zhou, Z. Y.; Wu, D. Y.; Ren, B.; Wang, Z. L.; Tian, Z. Q. *Nature* **2010**, *464*, 392.

(9) (a) Guerrero, A. R.; Aroca, R. F. *Angew. Chem., Int. Ed.* **2011**, *50*, 665. (b) Honesty, N. R.; Gewirth, A. A. *J. Raman Spectrosc.* **2012**, *43*, 46. (c) Xie, W.; Walkenfort, B.; Schlücker, S. *J. Am. Chem. Soc.* **2013**, *135*, 1657. (d) Graham, D. *Angew. Chem., Int. Ed.* **2010**, *49*, 9325. (e) Smith, S. R.; Leitch, J. J.; Zhou, C.; Mirza, J.; Li, S. B.; Tian, X. D.; Huang, Y. F.; Tian, Z. Q.; Baron, J. Y.; Choi, Y.; Lipkowski, J. *Anal. Chem.* **2015**, *87*, 3791.

(10) Barrios, C. A.; Malkovskiy, A. V.; Kisliuk, A. M.; Sokolov, A. P.; Foster, M. D. *J. Phys. Chem. C* **2009**, *113*, 8158.

(11) (a) Lakowicz, J. R.; Ray, K.; Chowdhury, M.; Szmacinski, H.; Fu, Y.; Zhang, J.; Nowaczyk, K. *Analyst* **2008**, *133*, 1308. (b) Geddes, C.; Lakowicz, J. *J. Fluoresc.* **2002**, *12*, 121. (c) Ming, T.; Chen, H.; Jiang, R.; Li, Q.; Wang, J. *J. Phys. Chem. Lett.* **2011**, *3*, 191. (d) Kinkhabwala, A.; Yu, Z.; Fan, S.; Avlasevich, Y.; Mullen, K.; Moerner, W. E. *Nat. Photonics* **2009**, *3*, 654. (e) Tam, F.; Goodrich, G. P.; Johnson, B. R.; Halas, N. J. *Nano Lett.* **2007**, *7*, 496. (f) Akselrod, G. M.; Argyropoulos, C.; Hoang, T. B.; Ciracì, C.; Fang, C.; Huang, J.; Smith, D. R.; Mikkelsen, M. H. *Nat. Photonics* **2014**, *8*, 835.

(12) Aslan, K.; Wu, M.; Lakowicz, J. R.; Geddes, C. D. *J. Am. Chem. Soc.* **2007**, *129*, 1524.

DOI: 10.1021/jacs.5b09682
J. Am. Chem. Soc. 2015, 137, 13784−13787